Macromolecules

Article

pubs.acs.org/Macromolecules

Intrinsic Stresses in Thin Glassy Polymer Films Revealed by Crack Formation

Mithun Chowdhury,[†,¶] Xiaoyuan Sheng,[§,∥,¶] Falko Ziebert,[†,⊥] Arnold C.-M. Yang,[#] Alessandro Sepe,[§] Ullrich Steiner,[*,§] and Günter Reiter[*,†,‡]

[†]Physikalisches Institut and [‡]Freiburger Materialforschungszentrum, Albert-Ludwigs-Universität, 79104 Freiburg, Germany
[§]Adolphe Merkle Institute, Chemin des Verdiers, 1700 Fribourg, Switzerland
[∥]Cavendish Laboratory, University of Cambridge, Cambridge CB3 0HE, United Kingdom
[⊥]Institut Charles Sadron UPR22-CNRS, 67034 Strasbourg, Cedex 2, France
[#]Department of Materials Science and Engineering, National Tsing Hua University, Hsinchu, Taiwan

Supporting Information

ABSTRACT: Both spin-coating and thermal annealing of thin supported glassy polymer films generally cause stresses arising from rapid solvent evaporation and from a mismatch in expansivities of film and substrate, respectively. While films on adhesive surfaces are typically stable, on slippery substrates film stability is sensitively determined by the thermal protocol, revealing the presence of these stresses. There, contraction of the film upon cooling causes in-plane tensile stresses that can lead to film fracture. While this is a general effect, the details of the film's response to thermal cycling allow to disentangle the origin of stresses within the film. For high molecular weight polymers, we found that preparation-induced stresses cause substantially reduced thermal expansivities. This demonstrates that intrinsic out-of-equilibrium states in spin-coated glassy films of long polymers are long-lived and thus difficult to equilibrate.

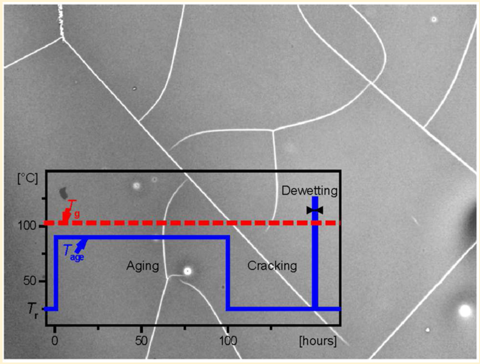

INTRODUCTION

The occurrence of stresses in micrometer thick polymer coatings caused by thermal protocols[1] is a well-studied problem. In supported films, strongly adhering to a solid substrate, a difference in the thermal expansion coefficients of the film and the substrate may produce significant stresses when varying the sample temperature.[2−4] To avoid film cracking or delamination, engineers typically aim to minimize such stresses.

A second source of stresses has been found, more recently, in thin nanometric polymer films. There is growing evidence[5,6] that thin glassy polymer films are not in thermodynamic equilibrium because their equilibration times are not experimentally accessible. Nonequilibrated chain conformations—typically generated by the rapid transition from a dilute solution to the dry glass caused by solvent evaporation during spin-coating—result in long-lived residual stresses *inside* the polymeric films. Interestingly, the out-of-equilibrium conformations on the level of chains have consequences on the macroscopic scale such as an accelerated dewetting dynamics[7] and in electrohydrodynamic instabilities.[8] The residual stresses have been evidenced by surface wrinkling,[9] cantilever deflection experiments,[10] and dewetting experiments, where they have been investigated in terms of polymer molecular weight, solvent quality, and aging time.[11−13]

A further consequence of reduced chain equilibration is differences in the entangled nature of the polymer chains. A reduction in entanglements has direct consequences on the toughness of the material and on its deformation or fracture mechanisms, since these properties are strongly dependent on the chain entanglement density.[14−18] While direct mechanical testing is difficult in thin films, several publications suggest anomalous mechanical properties in confinement, such as a reduced dependence of the elastic modulus on the polymer molecular weight,[17] a changed scaling of viscosity with molecular weight,[16] and accelerated deformation.[16] Despite this evidence, thin supported polymer films are often assumed to be close to thermodynamic equilibrium.

While considerable work was done on molecular mechanisms of localized deformations caused by external stresses (crazing and cracking), there are few similar experimental studies on ultrathin films, where the molecular size becomes comparable to the film thickness. These types of experiments are likely to reveal intrinsic residual stresses arising from frozen-in nonequilibrated chains which impact the stability, deformation, and failure in thin polymer films.

Received: August 9, 2016
Revised: November 7, 2016
Published: November 29, 2016

DOI: 10.1021/acs.macromol.6b01640
Macromolecules 2016, 49, 9060−9067

In this article, we examine the interplay of the two sources of stress described above: thermal mismatch and residual stress. We have applied a systematic thermal protocol to thin glassy polymers films spin-cast onto a slippery substrate and determined properties of cracks induced in the films through this protocol (Figure 1). In particular, we compare glassy films made of small (short chain) molecules with films made from long polymer chains. In the latter, preparation-induced stresses that vary with molecular weight, solvent quality, and aging time were shown to be significant.[11−13,19] A comparison of cracks formed in these two systems therefore enables conclusions about film preparation-induced stresses and their decay. The detection of cracking was corroborated by changes in film thickness detected by X-ray reflectometry.

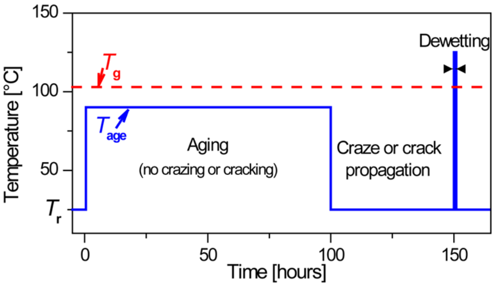

Figure 1. Schematic of the thermal protocol used: PS films were spin-cast at T_r and heated to T_{age} below T_g (dashed) for times t_{age}. For sufficiently long t_{age}, cooling back to T_r induced cracking/crazing. After allowing the cracks to propagate, the film was heated to 125 °C > T_g to induce dewetting.

RESULTS AND DISCUSSION

As a model polymer, we used the frequently studied polystyrene (PS) with various molecular weights (M_w): 49 kg/mol (polydispersity M_w/M_n = 1.03), 52 kg/mol (M_w/M_n = 1.07), 4060 kg/mol (M_w/M_n = 1.15), 4410 kg/mol (M_w/M_n = 1.15), and 16 800 kg/mol (M_w/M_n = 1.33). The 40−55 nm thick films were spin-cast from toluene (an athermal solvent for PS) and from *trans*-decalin (a Θ-solvent for PS) at room temperature onto smooth silicon wafers coated with a thin (≃15 nm) polydimethylsiloxane (PDMS) layer.[7] The PDMS layer provides a well-defined surface of low interfacial friction characterized by a large slippage length for PS.[7]

Cracking was studied by imposing the temperature protocol shown in Figure 1. The films were heated from room temperature T_r to an aging temperature T_{age} below the bulk glass transition temperature $T_g \simeq 105$ °C and kept there for an aging time t_{age} to (partially) relax stresses in the film induced by spin-coating and thermal expansion.[11,13] Aging was performed in an oil-free vacuum oven or in a Linkam hot stage. After aging, the films were rapidly[20] cooled to T_r. For high enough T_{age} and long enough t_{age}, this induced crack formation in the films.

Figure 2a shows the formation of cracks in low-M_w PS films. Cracks cut across the thickness of the entire film and initially grew at about 5−10 μm/s. Crack tips approaching previously formed cracks slowed down and changed propagation direction for the two cracks to meet at a right angle (e.g., crack 2 merging with crack 1 in Figure 2a; see also Supporting Information). This behavior arises from locally relaxed stress regions in the vicinity of already formed cracks.[4]

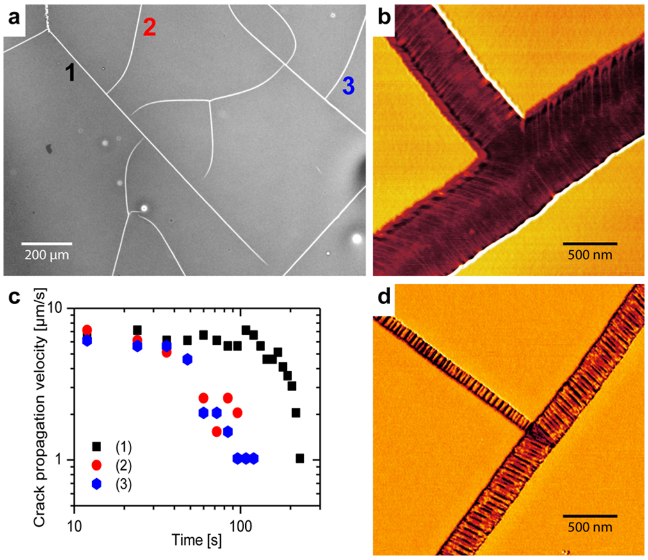

Figure 2. (a) Optical micrograph of cracks in a low-M_w PS film (52 kg/mol, 55 nm thick, t_{age} = 24 h at 90 °C). Younger cracks (2) join older ones (1) at right angles. (b) High-resolution image of a "crack" junction that has formed in a 48 nm thick film of M_w = 52 kg/mol PS film aged for 24 h at 90 °C. The very thin fibrillar structure are fragile crazes that have partially failed during the crack-opening process. (c) Propagation velocities of the cracks labeled in (a). (d) AFM phase image of a typical craze junction in a high-M_w film (4060 kg/mol, 40 nm thick, t_{age} = 40 days at 90 °C) that is spanned by a characteristic fibrillar structure. The wider craze has formed first.

The cracks displayed the typical crazes, i.e., cracks bridged by a fibrillar substructure,[21−25] shown in the AFM image in Figure 2b,d. Above the entanglement molecular weight $M_e \approx 17$ kg/mol, crack formation involves the formation of crazes in the crack tip, but for $M_w \gtrsim M_e$ the crazes are fragile and fail upon crack opening. Thus, crazes are difficult to detect experimentally for $M_w \gtrsim M_e$ but clearly visible for $M_w \gg M_e$ (Figure 2b,d).[26] To help to distinguish crack formation in high- and low-M_w PS films, we refer to the structures in Figure 2b,d as "cracks" and "crazes", respectively. Despite these differences in the appearance, the molecular mechanisms of crack formation is very similar for the whole range of molecular weights used in this study.

A detailed investigation of the morphological features within cracks and crazes (width, depth, fibril and void sizes) can shed light on the balance of stress and fracture toughness within the films.[21−23,25,27,28] Figure 3 shows that crazes did not penetrate the entire film thickness, whereas cracks cut across the entire film thickness (Figure 3b−d). Crazes are characterized by a dense fibril structure in thick films (Figure 3e), while they resemble a perforated sheet in thinner films (Figure 3a,f) caused by a reduction in out-of-plane plastic strain. For both cracks and crazes, the width increases linearly with film thickness, leveling off at ≈100 nm. Interestingly, the crack width extrapolates to zero at a film thickness of 30 nm (Figure 3d), which corresponds to the threshold below which films are stable, irrespective of molecular weight. Large crack widths and high fracture toughness G_c are common in thick films, in agreement with linear elastic fracture mechanics,[3,4,29] although simple models underestimate the fracture energy for highly entangled polymers caused by localized yielding process such as the formation of stable crazes.[14,26−28] In general, large craze widths and small fibril/void diameters are indicative of high

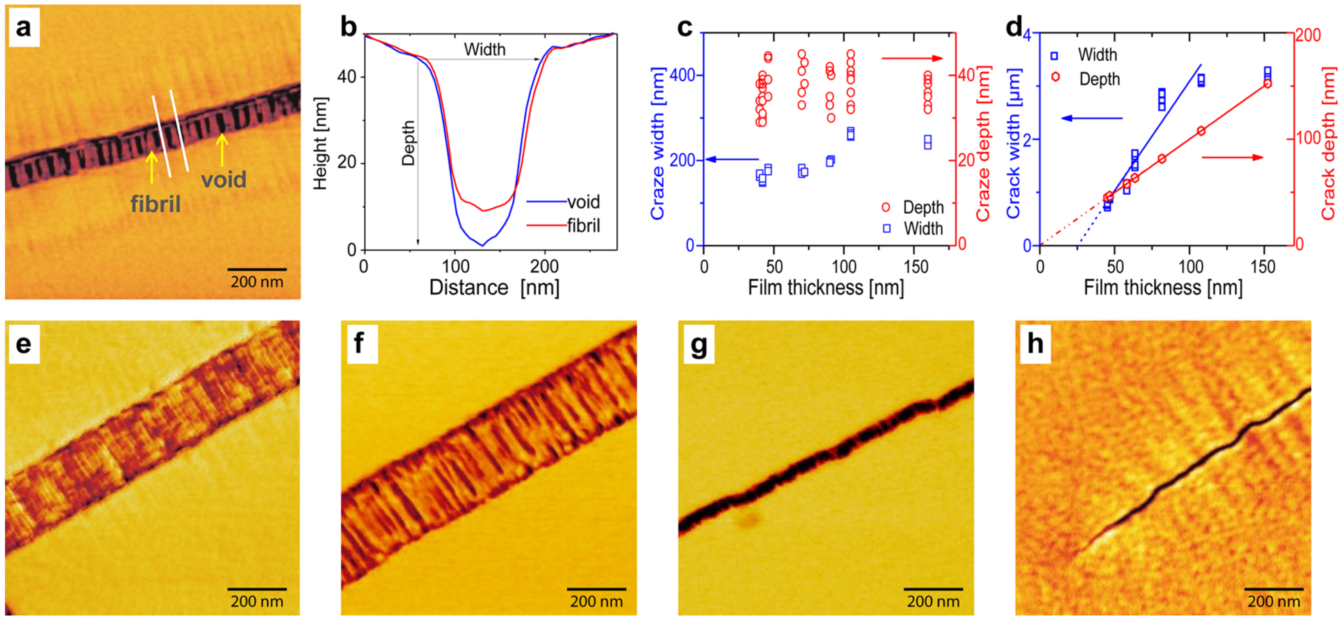

Figure 3. (a, e−h) AFM phase images showing a comparison of typical craze microstructures in high-M_w PS films. (a) Typical craze pattern in a PS film consisting of separated voids and fibrils. (b) Height profiles across a craze at the positions of a void and a fibril, indicated by white lines in (a). (c, d) Variation of width and depth of crazes/cracks with h. Crazes do not penetrate the entire film, whereas cracks cut across the entire film. The latter leads to a slope of 1 in the crack depth vs h plot. Cracks were formed in low-M_w PS, whereas crazes were formed in high-M_w films. Crazes in (e) a 90 nm thick PS film, (f) a PS film aged for 40 days, and (g) a PS film spun from *trans*-decalin. (h) Craze tip in the film of (a). Unless otherwise specified, all films were cast from toluene, had a thickness of ∼40 nm, and were aged at 90 °C for 24 h.

crazing stresses, which give rise to high fibril nucleation densities behind the advancing crack tip.[22,27,28,30] Also, the fracture toughness is primarily limited by the craze width, which depends on the maximum crazing stress which the craze fibril can withstand.[27,28] Note that cracks and crazes that formed at late stages of experiments were not considered and crack morphological parameters were always measured in the middle of long isolated cracks, far from the crack tip, or crack intersections (i.e., avoiding regions like the one shown in Figure 3h).

Films spun from *trans*-decalin (a near-Θ-solvent for PS at room temperature[12]) show narrower crazes when exposed to the thermal protocol of Figure 1 compared to films prepared from the good solvent toluene (compare Figures 3a and 3g). Lower craze widths and reduced craze propagation velocities indicate lower crazing stresses in the former. This is indicative of higher in-plane stresses in films spun from toluene, compared to *trans*-decalin, arising from differences in polymer coil deformations in the as-cast films.[12] Aging these films relaxes these stresses.[12,13] This is witnessed in dewetting experiments of aged films, where the dewetting velocity decreases with aging time, particularly in high-M_w films (Figure 4).

Pronounced differences in the growth kinetics of cracks and crazes were observed. Figure 5a compares crack and craze propagation velocities (v_{crack}, v_{craze}) in films of PS of three different molecular weights that were aged for increasing periods t_{age} according to the protocol of Figure 1. While v_{crack} in films of 52 kg/mol PS was constant at ∼10 μm/s, independent of t_{age}, v_{crack} in the two high-M_w PS films was 2 orders of magnitude lower for small aging times but increased with t_{age} to reach the value for the low-M_w film after t_{age} ∼ 10^3 h. High- and low-M_w films differed also in terms of the total length of all cracks or crazes in a given sample area as a function of t_{age}, shown in Figure 5b. While the total length of all cracks per area did not change with t_{age} in low-M_w films, the total length of crazes increased with aging time in high-M_w films, approaching the value of low-M_w cracks for t_{age} ∼ 70 h.

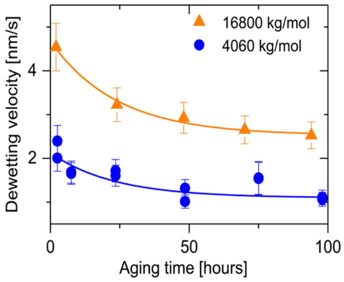

Figure 4. Variation of the dewetting velocity of high-M_w samples, recorded 1000 s after the initiation of dewetting by heating the sample to 125 °C. The lines are exponential fits to the data, yielding a decay rate of 7 ± 2 h. The variation in dewetting speed was more pronounced for the high-M_w sample.

High in-plane tensile stresses drive the propagation of cracks and crazes in polymer films, with propagation velocities that are governed by the energy release rate G_c.[22] The variation of G_c with polymer molecular weight is well established for the bulk. G_c increases for values of the molecular weight higher than M_e and levels off at ca. 8−10 M_e.[14,26,28,31] In confinement, however, the $G_c - M_w$ variation is likely to be different because of a reduction in entanglements and an increased role of the surrounding boundaries.[15,17,18] For the molecular weights and film thicknesses used in this study, the variation in G_c is likely to be small, approximately a factor of 2.[17]

In the quasi-static regime of subcritical, slow crack-propagation, the crack opening velocity is thermally activated and scales with G_c.[32] The initial reduction in v_{craze} of the high-M_w PS film in Figure 5a is, however, much larger, i.e., more than 2 orders of magnitude. This implies a substantial *reduction* in the total in-plane stresses compared to low-M_w films.

DOI: 10.1021/acs.macromol.6b01640
Macromolecules 2016, 49, 9060−9067

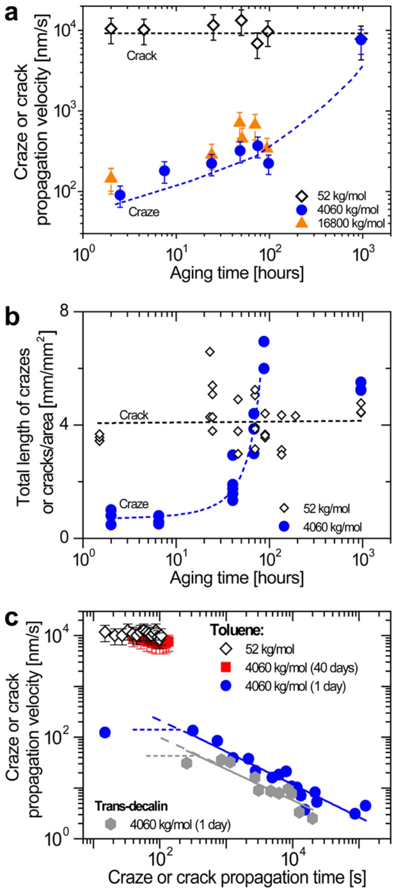

Figure 5. (a) Crack and craze propagation velocities (measured ≃100 s after nucleation) as a function of aging time for three M_ws. The dashed lines are guides to the eye. (b) Total length of cracks/crazes per unit area as a function of aging time for two M_ws. (c) Time-resolved craze and crack propagation velocities. Crazes in high-M_w films aged for 24 h decelerated with time. All low-M_w films and high-M_w films that were aged for 40 days had high propagation velocities that formed a complete crack pattern within 2 h. All films were ≈40 nm thick and were aged at T_{age} = 90 °C.

Intriguingly, these driving stresses *increased* with aging time, although residual stresses relax upon aging.

In sufficiently aged high-M_w films, crazes propagated with ~10^4 nm/s (i.e., driven by the same maximum in-plane stress as for the low-M_w sample). This velocity remained constant until the final craze pattern had formed. For short aging times, however, v_{craze} in high-M_w films decelerated with increasing propagation time, as shown in Figure 5c. This regime was additionally influenced by the solvent from which the film was cast because of its influence on the nonequilibrium chain conformations.[12] Films prepared from *trans*-decalin (a Θ-solvent) showed consistently lower values of v_{craze} compared to films cast from toluene (an athermal solvent). Films prepared from both solvents showed however a similar deceleration in v_{craze} with propagation time (Figure 5c).

Note that in our system crack/craze formation in thin PS films is subject to two key requirements. First, slip between the incompatible PS film and the PDMS substrate layer is crucial. Control experiments using PS films on unmodified silicon substrates, i.e., with adhesive interactions, never showed crack formation. Second, crack/craze formation requires aging the samples for sufficiently long times at sufficiently high aging temperatures $T_{age} < T_g$. Film failure was only observed above a critical value of T_{age}, with $T_{age}^{min} = T_g - (20 \pm 5)$ °C and $T_{age}^{min} = T_g - (30 \pm 5)$ °C for the highest and the lowest M_w, respectively.

The three measurements in Figures 2c, 4, and 5a,b probe different relaxation mechanisms (cracking, dewetting), which presumably probe a different interplay of interfacial slip and aging. Remarkably, the overall relaxation times in all experiments are on the order of magnitude of 100 h (perhaps with the exception of Figure 5a, where data in the 100−1000 h interval was not acquired).

The observations of Figure 5 can be interpreted in terms of an interplay of stresses arising both from film preparation, thermal expansivity, and slip. Heating a PS film on a silicon wafer to T_{age} causes thermal expansion of the film and thereby a compressive thermal mismatch stress[3] $\sigma_{th}^{heat} > 0$ whose maximum is given for a perfectly sticking film by

$$\sigma_{th}^{max} = \overline{E}_f \Delta\alpha \Delta T \qquad (1)$$

where $\overline{E}_f = E_f/(1 - \nu_f)$ is the effective elastic modulus of the polymer film and $\Delta T = T_{age} - T_r$. $\Delta\alpha = \alpha_f - \alpha_s$, with $\alpha_f \simeq 7 \times 10^{-5}$/K and $\alpha_s \simeq 2.5 \times 10^{-6}$/K the thermal expansion coefficients of the film and the substrate, respectively.[33,34]

Assuming the absence of interfacial slip, $\sigma_{th}^{heat} = \sigma_{th}^{max} \simeq 24$ MPa, using E_f = 3.7 GPa, a Poisson ratio ν_f = 0.33,[9,33] and ΔT = 65 K. This stress is not sufficiently high to cause delamination or buckling, which typically requires stresses on the order of the elastic modulus.[4,35] Cooling back to room temperature inverts the thermal expansion, returning the film to its initial state.

In the presence of interfacial slip on the PDMS-covered substrate, σ_{th}^{heat} can be (partially) relaxed. If the sample is kept at T_{age} for a sufficiently long time, lateral expansion by slipping releases the temperature induced compressive stress. Rapid cooling then induces uniaxial film contraction, thereby causing an in-plane tensile stress σ_{th}^{cool} through the thermal mismatch of substrate and film. For short aging times, this stress (partially) compensates for the compressive stress σ_{th}^{heat} induced by the previous temperature increase, but if the film is stress-free at T_{age}, $\sigma_{th}^{cool} = -\sigma_{th}^{heat}$.

While the tensile strength of bulk PS is in the 46−60 MPa range, it is reduced in very thin films.[21] In particular, a tensile strength of ≈20 MPa was reported for 50 nm thick PS films (M_w = 654 kg/mol) on a PDMS substrate.[36] The estimated value of eq 1 of 24 MPa therefore exceeds the film strength, leading to the observed cracking and crazing.

X-ray reflectometry (XR) measurements were carried out to confirm these model assumptions (see Supporting Information). As-cast low-M_w samples were mounted in the reflectometer, and the film thickness h was monitored during annealing at 90 °C, shown in Figure 6a (triangles). Upon heating, the film initially expanded, but with continued heating this was followed by a marked reduction in h. Cooling to T_r resulted in the expected thermal contraction in h, followed by a gradual increase. After 11 days a comparable value to the initial, as-cast film thickness was reached. This variation in h with time is in good agreement with the model assumptions above. Figure 6b illustrates the interplay of thermal expansion/contraction with lateral film slip and the evolution of stresses in the film. The return of h to its initial value indicates that as-cast low-M_w films seem to be reasonably well-equilibrated (in terms of their volume).

The thickness response of high-M_w films to the heating cycle shown in Figure 6a was qualitatively similar, with three significant differences. (1) Initial thermal expansion was much

DOI: 10.1021/acs.macromol.6b01640
Macromolecules 2016, 49, 9060−9067

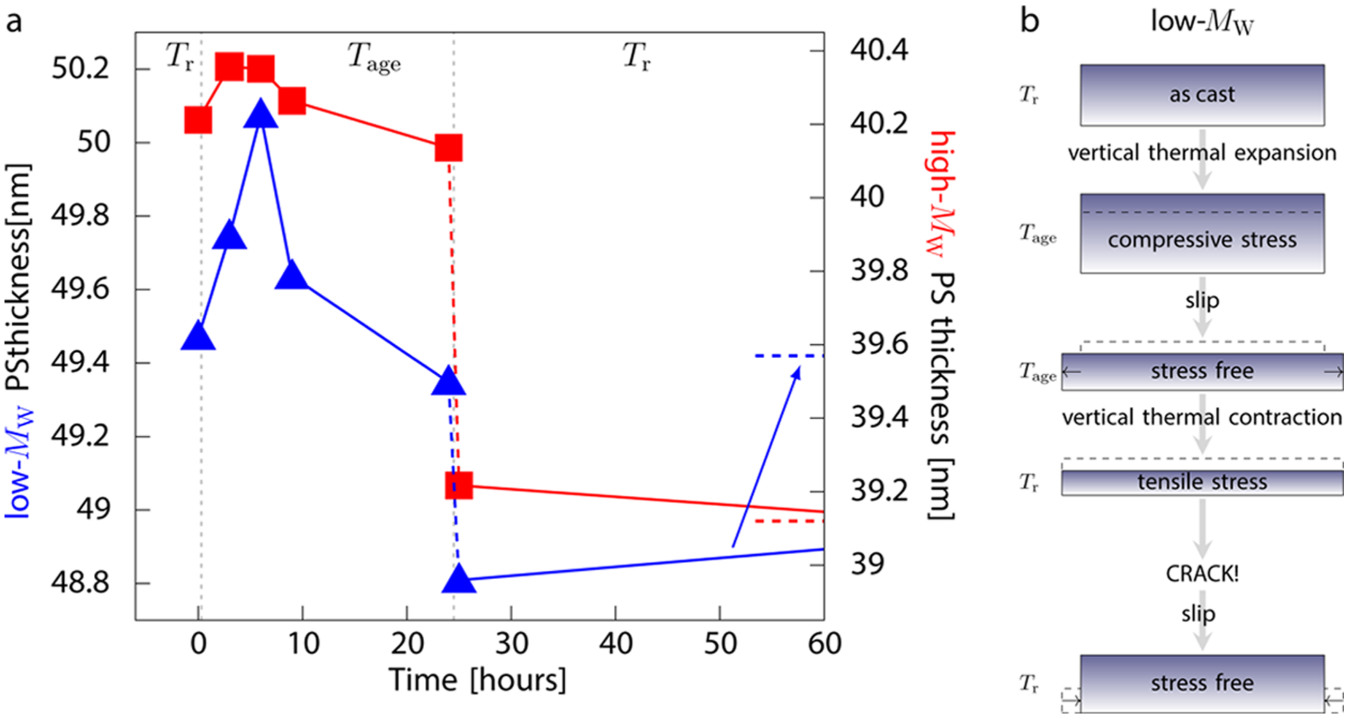

Figure 6. (a) Film thickness evolution measured by XR of low- and high-M_w PS films (triangles and squares, respectively) aged for 24 h at T_{age} = 90 °C followed by a quench to T_r. The point at 0 h is the as-cast thickness at T_r. The dashed horizontal lines are long-time values measured after 72 and 288 h for high- and low-M_w PS, respectively. See Supporting Information for XR data and an error analysis. The samples were thermally cycled using a Linkam stage (open lid). The heating rate was 50 K/min, and room temperature was reached within 20 min, when cooling. The very slow initial increase in film thickness in both films is probably due to slow chain relaxation mechanisms as described before.[37] (b) Schematic of the interplay of thermal expansion/contraction, interfacial slip, and the buildup and relaxation of stresses in the low-M_w film.

reduced compared to the low-M_w sample. This arises from the well-known negative expansivity of high molecular weight polymer films near the glass transition temperature.[38−41] While as-deposited films show negative expansion when heated to 95−105 °C, the expansion at 90 °C is very small.[38] (2) The subsequent film thickness contraction was also reduced. This reflects the much smaller expansion during heating, requiring less slip to relax the film, possibly combined with preparation-induced tensile stresses that compensate for the compressive stress caused by film expansion during heating.

While the decrease in film thickness upon quenching to T_r after 24 h is comparable to the low-M_w film, this is (3) followed by further gradual *decrease* in film thickness. In contrast to the low-M_w case, the thickness of high-M_w films after several days is much lower than the as-cast value. Clearly, in terms of their volume, as-cast high-M_w films are far from equilibrium with slow equilibration taking place even at temperatures much below T_g, as observed before.[5,8]

A model which is purely based on the stress of eq 1 and its relaxation by slip (Figure 6b) therefore adequately describes only low-M_w PS films, where chain conformations are not far from thermodynamic equilibrium after film-casting. This is however not the case for high molecular weights, where film formation may lead to a range of nonequilibrium phenomena.[42] In this case, thermally induced and residual stresses superpose,[10] and relaxation processes lead to a change in density.

The latter can lead to a much reduced thermal expansion of as-cast films. Depending on the protocol, even negative expansion coefficients (film thicknesses that decrease for increasing temperatures) have been observed,[38−41] attributed to residual solvent and nonequilibrium chain conformations introduced during film preparation. Both give rise to an excess film thickness of the as-cast film that only gradually decreases upon annealing or aging via solvent release and chain relaxation.

This effect is observed for the high-M_w polymer and leads to the reduced initial thermal expansion in Figure 6a. Additionally, a gradual decrease in the thickness of the high-M_w film over 72 h is discernible, covering all stages of the annealing protocol, confirming the extremely long time scales for high-M_w film aging. In contrast, the low-M_w film returns to approximately the initial thickness after the heating cycle and does not exhibit marked aging effects.

Film stability for $T_{age} < T_{age}^{min}$ probably arises from a combination of two effects, a reduced slippage for too low aging temperatures, and values of ΔT in eq 1 that give rise to values of tensile stresses σ_{th}^{max} that are lower than the PS tensile strength. Neglecting the first effect allows to estimate the stability limit. The lowest aging temperature for which cracks were observed in low-M_w films of T_{age}^{min} = 75 °C leads to a film strength of $\sigma_{th}^{max} \approx 19$ MPa, which is very close to the value reported in tensile-test experiments.[36] Note that slow cooling allows partial relaxation of the thermally induced tensile stress by slipping while the temperature decreases, leading to the formation of narrower cracks,[20] (see Supporting Information), in agreement with our interpretation above.

To account for the compensation of thermal expansion and residual stress relaxation, α_f in eq 1 has therefore to be replaced by an "effective" expansion coefficient $\alpha_f^{eff}(t_{age})$ containing thermal and preparation-induced contributions

DOI: 10.1021/acs.macromol.6b01640
Macromolecules 2016, 49, 9060−9067

$$\alpha_f^{\text{eff}}(t_{\text{age}}) = \frac{1}{T_{\text{age}} - T_r} \int_{T_r}^{T_{\text{age}}} \alpha_f[T, \sigma_{\text{res}}(t_{\text{age}})]\, dT \tag{2}$$

For low temperatures, molecular relaxation is slow (but possible) and increases for $T_{\text{age}} \to T_g$.[40,41] For a given T_{age}, α_f^{eff} is hence a function of t_{age} via the residual stress $\sigma_{\text{res}}(t_{\text{age}})$. Thermal expansion is small for as-cast films,[39−41] and α_f^{eff} increases with aging time and aging temperature, reflecting the increasing relaxation of the chains within the film. Obviously, this directly translates to a dependence of the thermal stresses on aging time and aging temperature through eq 1.

Since α_f^{eff} obtains a characteristic time scale from the residual stress and imparts it on the mismatch stress through eq 1, we can extract the characteristic time scale for the relaxation of residual stresses from Figure 5a. Assuming an exponential decay,[7] a characteristic time constant τ = 14 ± 8 h is determined for the 4060 kg/mol sample for aging times up to 100 h. This value is on the same order of magnitude as τ = 7 ± 2 h extracted from dewetting experiments at 125 °C,[13] which was confirmed here by initiating dewetting of films containing crazes (Figure 4). While the stress decay takes place on the time scale of several hours, structural relaxation processes that result in a volume change are slower (several days) as discernible in Figure 6.

Returning to the results of Figure 5, upon cooling from T_{age} a lower value of α_f^{eff} results in lower (but still substantial) tensile stresses, as borne out by the reduced craze propagation velocities in Figure 5a. Maintaining the sample over many tens of hours at T_{age} caused equilibration of the high-M_w films, and the subsequent film instability approached that of the low-M_w films (Figure 5a). The same applies to the areal craze density in Figure 5b, where a lower effective tensile stress reduced the probability of nucleation of crazes. In addition, the reduction in craze propagation with time (Figure 5c) prevented the completion of a final craze pattern, yielding a lowered areal craze density.

Low in-plane stresses in quenched high-M_w films also explain the result of Figure 5c. For high crack propagation velocities, a complete crack pattern is formed on time scales of only a few minutes, much shorter than the time over which the film is able to laterally contract by slippage. The much lower craze propagation velocities found for high-M_w films (Figure 5a) significantly extend the time over which crazing occurs (up to several days), thus increasing the time period for in-plane slippage of the entire film, which in turn progressively lowers in-plane stresses that drive craze propagation. This gives rise to the slowdown observed in Figure 5c. The results of Figure 5c also compare well with controlled dewetting studies[7,13] of identically prepared films that showed a decrease of tensile residual stresses in high-M_w films with aging. Finally, the lateral offset of the two data sets in Figure 5c prepared from two different solvents indicates a difference in preparation-induced in-plane tensile stresses as discussed before.[19]

Note that while preparation induced stresses in high-M_w films can be substantial,[19] these stresses typically are balanced by the adhesion to the substrate. Homogenous adhesion inhibits crack nucleation, rendering the films stable upon their initial manufacture. Rapid, nonadiabatic temperature changes may however induce density fluctuations, which can nucleate cracks, as described here.

The results of Figure 5 are reminiscent of the well established embrittlement of polymers in bulk samples. The deformation of samples during mechanical testing induces enhanced ductility, which fades upon aging, thereby “embrittling” the sample.[43] Microscopically, this is likely caused by a local reorganization of chain conformations, which reduces stored stresses and perhaps re-entangles the polymers. While this needs to be further investigated, it is possible that the increase in craze velocity in Figure 5 (effectively *embrittling* the films) and the embrittlement in mechanically deformed bulk samples may be linked. In both cases, thermal aging relaxes (nonequilibrium) molecular chain conformations, leading to a partial recovery of the mechanical properties of the sample.

■ CONCLUSION

Nonequilibrium chain conformations and their relaxation in thin polymer films induce rather intricate effects that are often difficult to access directly in experiments. However, the interplay between thermal and preparation-induced stresses combined with film slip at the substrate induces cracks and crazes that are easy to observe by optical microscopy. Cooling low-M_w PS films causes a reduction in film thickness, which gives rise to a large in-plane tensile stress that is directly responsible for crack formation and propagation. Upon cooling high-M_w films, craze formation and propagation sensitively depend on the thermal history of the film. The study of craze formation and propagation is therefore a novel method to investigate the relaxation toward equilibrium of thin polymer films.

Our study showed that stresses in thin films can efficiently be relaxed by aging on slippery substrates, ultimately yielding effectively *stress-free* films. These experiments are fundamentally different from the case of polymers strongly adhering to common substrates (e.g., silicon wafers), where slip between the polymer and the substrate is nearly impossible.[44] While this suppresses cracking, it also inhibits the relaxation toward stress-free films. As a consequence, and contrary to frequent statements, removal of in-plane stresses is difficult to achieve by annealing films on adhesive substrates, since cooling to room temperature inevitably generates substantial tensile stresses which may affect macroscopic properties of the material.

■ ASSOCIATED CONTENT

Supporting Information

The Supporting Information is available free of charge on the ACS Publications website at DOI: 10.1021/acs.macromol.6b01640.

Figures 1−6 and Tables 1 and 2 (PDF)

■ AUTHOR INFORMATION

Corresponding Authors

*E-mail: ullrich.steiner@unifr.ch (U.S.).

*E-mail: guenter.reiter@physik.uni-freiburg.de (G.R.).

ORCID

Ullrich Steiner: 0000-0001-5936-339X

Present Address

M.C.: Department of Chemical and Biological Engineering, Princeton University, Princeton, NJ 08544.

Author Contributions

[¶]M.C. and X.S. made equal contributions.

Notes

The authors declare no competing financial interest.

■ ACKNOWLEDGMENTS

We thank the Deutsche Forschungsgemeinschaft (RE2273/3-1 & IRTG 1642 Soft Matter Science), the EPSRC (EP/E022561), and the Adolphe Merkle Foundation for funding. We acknowledge the support from the Winton Programme for the Physics of Sustainability.

■ REFERENCES

(1) Tong, H. M.; Hu, C.-K.; Feger, C.; Ho, P. S. Stress Development in Supported Polymer Films During Thermal Cycling. *Polym. Eng. Sci.* **1986**, *26*, 1213.

(2) Chung, J. Y.; Lee, J.-H.; Beers, K. L.; Stafford, C. M. Stiffness, Strength, and Ductility of Nanoscale Thin Films and Membranes: A Combined Wrinkling-Cracking Methodology. *Nano Lett.* **2011**, *11*, 3361−3365.

(3) Freund, L. B.; Suresh, S. *Thin Film Materials: Stress, Defect Formation and Surface Evolution*; Cambridge University Press: Cambridge, 2003.

(4) Hutchinson, J. W.; Suo, Z. Mixed Mode Cracking in Layered Materials. *Adv. Appl. Mech.* **1991**, *29*, 63.

(5) Napolitano, S.; Wübbenhorst, M. The lifetime of the deviations from bulk behaviour in polymers confined at the nanoscale. *Nat. Commun.* **2011**, *2*, 260.

(6) Napolitano, S.; Rotella, C.; Wübbenhorst, M. Can Thickness and Interfacial Interactions Univocally Determine the Behavior of Polymers Confined at the Nanoscale? *ACS Macro Lett.* **2012**, *1*, 1189.

(7) Reiter, G.; Hamieh, M.; Damman, P.; Sclavons, S.; Gabriele, S.; Vilmin, T.; Raphaël, E. Residual stresses in thin polymer films cause rupture and dominate early stages of dewetting. *Nat. Mater.* **2005**, *4*, 754.

(8) Barbero, D. R.; Steiner, U. Nonequilibrium Polymer Rheology in Spin-Cast Films. *Phys. Rev. Lett.* **2009**, *102*, 248303.

(9) Chung, J. Y.; Chastek, T. Q.; Fasolka, M. J.; Ro, H. W.; Stafford, C. M. Quantifying Residual Stress in Nanoscale Thin Polymer Films via Surface Wrinkling. *ACS Nano* **2009**, *3*, 844.

(10) Thomas, K. R.; Steiner, U. Direct stress measurements in thin polymer films. *Soft Matter* **2011**, *7*, 7839−7842.

(11) Damman, P.; Gabriele, S.; Coppée, S.; Desprez, S.; Villers, D.; Vilmin, T.; Raphaël, E.; Hamieh, M.; Akhrass, S. A.; Reiter, G. Relaxation of Residual Stress and Reentanglement of Polymers in Spin-Coated Films. *Phys. Rev. Lett.* **2007**, *99*, 036101.

(12) Raegen, A.; Chowdhury, M.; Calers, C.; Schmatulla, A.; Steiner, U.; Reiter, G. Aging of Thin Polymer Films Cast from a Near-Theta Solvent. *Phys. Rev. Lett.* **2010**, *105*, 227801.

(13) Chowdhury, M.; Freyberg, P.; Ziebert, F.; Yang, A. C.-M.; Steiner, U.; Reiter, G. Segmental Relaxations have Macroscopic Consequences in Glassy Polymer Films. *Phys. Rev. Lett.* **2012**, *109*, 136102.

(14) Dai, C.-A.; Kramer, E. J.; Washiyama, J.; Hui, C.-Y. Fracture toughness of polymer interface reinforced with diblock copolymer: effect of homopolymer molecular weight. *Macromolecules* **1996**, *29*, 7536−7543.

(15) Si, L.; Massa, M. V.; Dalnoki-Veress, K.; Brown, H. R.; Jones, R. A. Chain entanglement in thin freestanding polymer films. *Phys. Rev. Lett.* **2005**, *94*, 127801.

(16) Rowland, H. D.; King, W. P.; Pethica, J. B.; Cross, G. L. Molecular confinement accelerates deformation of entangled polymers during squeeze flow. *Science* **2008**, *322*, 720−724.

(17) Isaacson, S. G.; Lionti, K.; Volksen, W.; Magbitang, T. P.; Matsuda, Y.; Dauskardt, R. H.; Dubois, G. Fundamental limits of material toughening in molecularly confined polymers. *Nat. Mater.* **2015**, *15*, 294−298.

(18) Liu, Y.; Chen, Y.-C.; Hutchens, S.; Lawrence, J.; Emrick, T.; Crosby, A. J. Directly Measuring the Complete Stress-Strain Response of Ultrathin Polymer Films. *Macromolecules* **2015**, *48*, 6534−6540.

(19) Thomas, K. R.; Chenneviere, A.; Reiter, G.; Steiner, U. Nonequilibrium behavior of thin polymer films. *Phys. Rev. E* **2011**, *83*, 021804.

(20) Rapid cooling was typically performed by removing the sample from the oven. To test the influence of the cooling rate, slower cooling of low-M_w films was also investigated. Slower cooling resulted in a reduction of the crack width and a decrease in the total length of cracks formed per area. This also implies a reduction in the time-integrated propagation velocity (see Supporting Information).

(21) Chan, T.; Donald, A.; Kramer, E. Film thickness effects on craze micromechanics. *J. Mater. Sci.* **1981**, *16*, 676−686.

(22) Kramer, E. J. Microscopic and moelcular fundamentals of crazing. *Adv. Polym. Sci.* **1983**, *52*, 1.

(23) Lin, J.-H.; Yang, A. C.-M. Crazing Micromechanism in Glassy Atactic Polystyrene and Its Blends with Poly(2,6-dimethyl-1,4-diphenyl oxides) by AFM. *Macromolecules* **2001**, *34*, 3698.

(24) McGraw, J. D.; Fowler, P. D.; Ferrari, M. L.; Dalnoki-Veress, K. Relaxation of non-equilibrium entanglement networks in thin polymer films. *Eur. Phys. J. E: Soft Matter Biol. Phys.* **2013**, *36*, 7.

(25) Crosby, A. J.; Fasolka, M. J.; Beers, K. L. High-Throughput Craze Studies in Gradient Thin Films Using Ductile Copper Grids. *Macromolecules* **2004**, *37*, 9968.

(26) Kramer, E. A molecular theory of the fracture toughness of low molecular weight polymers. *J. Mater. Sci.* **1979**, *14*, 1381−1388.

(27) Brown, H. A molecular interpretation of the toughness of glassy polymers. *Macromolecules* **1991**, *24*, 2752−2756.

(28) Rottler, J.; Barsky, S.; Robbins, M. O. Cracks and crazes: on calculating the macroscopic fracture energy of glassy polymers from molecular simulations. *Phys. Rev. Lett.* **2002**, *89*, 148304.

(29) Leung, K.-t.; Néda, Z. Pattern formation and selection in quasistatic fracture. *Phys. Rev. Lett.* **2000**, *85*, 662.

(30) Donald, A. M.; Chan, T.; Kramer, E. J. The effect of film thickness on craze microstructure. *J. Mater. Sci.* **1981**, *16*, 669.

(31) Mikos, A. G.; Peppas, N. A. Polymer chain entanglements and brittle fracture. *J. Chem. Phys.* **1988**, *88*, 1337−1342.

(32) Lengliné, O.; Toussaint, R.; Schmittbuhl, J.; Elkhoury, J. E.; Ampuero, J. P.; Tallakstad, K. T.; Santucci, S.; Måløy, K. J. Average crack-front velocity during subcritical fracture propagation in a heterogeneous medium. *Phys. Rev. E* **2011**, *84*, 036104.

(33) Brandrup, J., Immergut, E. H., Grulke, E. A., Eds.; *Polymer Handbook*, 4th ed.; Wiley: New York, 1999.

(34) Linde, D. R., Ed.; *CRC Handbook of Chemistry and Physics*, 4th ed.; CRC Press: Boca Raton, FL, 2000.

(35) Closa, F.; Ziebert, F.; Raphaël, E. Interplay of internal stresses, electric stresses, and surface diffusion in polymer films. *Phys. Rev. E* **2011**, *83*, 051603.

(36) Lee, J.-H.; Chung, J. Y.; Stafford, C. M. Effect of Confinement on Stiffness and Fracture of Thin Amorphous Polymer Films. *ACS Macro Lett.* **2012**, *1*, 122−126.

(37) Reiter, G.; De Gennes, P. G. Spin-cast, thin, glassy polymer films: Highly metastable forms of matter. *Eur. Phys. J. E: Soft Matter Biol. Phys.* **2001**, *6*, 25−28.

(38) Kanaya, T.; Miyazaki, T.; Inoue, R.; Nishida, K. Thermal expansion and contraction of polymer thin films. *Phys. Status Solidi B* **2005**, *242*, 595−606.

(39) Orts, W. J.; van Zanten, J. H.; Wu, W.-l.; Satija, S. K. Observation of temperature dependent thicknesses in ultrathin polystyrene films on silicon. *Phys. Rev. Lett.* **1993**, *71*, 867−870.

(40) Miyazaki, T.; Nishida, K.; Kanaya, T. Contraction and reexpansion of polymer thin films. *Phys. Rev. E* **2004**, *69*, 022801.

(41) Mukherjee, M.; Bhattacharya, M.; Sanyal, M. K.; Geue, T.; Grenzer, J.; Pietsch, U. Reversible negative thermal expansion of polymer films. *Phys. Rev. E: Stat. Phys., Plasmas, Fluids, Relat. Interdiscip. Top.* **2002**, *66*, 061801.

(42) Sheng, X.; Wintzenrieth, F.; Thomas, K. R.; Steiner, U. Intrinsic viscoelasticity in thin high-molecular-weight polymer films. *Phys. Rev. E* **2014**, *89*, 062604.

(43) Van Melick, H.; Govaert, L.; Raas, B.; Nauta, W.; Meijer, H. Kinetics of ageing and re-embrittlement of mechanically rejuvenated polystyrene. *Polymer* **2003**, *44*, 1171−1179.

(44) Napolitano, S.; Capponi, S.; Vanroy, B. Glassy dynamics of soft matter under 1D confinement: How irreversible adsorption affects

molecular packing, mobility gradients and orientational polarization in thin films. *Eur. Phys. J. E: Soft Matter Biol. Phys.* **2013**, *36*, 61.

DOI: 10.1021/acs.macromol.6b01640